On the spectral dependency of UV radiation enhancements due to clouds in Valdivia, Chile (39.8°S)

Charlotte Lovengreen
Instituto de Física, Universidad Austral de Chile, Valdivia, Chile

Humberto A. Fuenzalida
Departamento de Geofísica, Facultad de Ciencias Físicas y Matemáticas, Universidad de Chile, Santiago, Chile

Leonardo Videla
Departamento de Ingeniería Matemática, Facultad de Ciencias Físicas y Matemáticas, Universidad de Chile, Santiago, Chile

Received 20 August 2004; revised 13 January 2005; accepted 25 February 2005; published 27 July 2005.

[1] Data gathered with a five-channel radiometer are used to analyze the spectral composition of cloud enhancements and attenuations of UV (305, 320, 340, and 380 nm) and photosynthetically active radiation (PAR) (400–700 nm) at Valdivia, Chile (39.8°S), during summer months and within 3 hours from solar noon. Variations are referred to clear-sky days occurring at not too distant dates or obtained as polynomial fit to cloud-free periods on partially cloudy days. Photographic images of the sky were taken simultaneously with part of the radiometric data. Frequency of occurrence and duration of enhancements were estimated. Most of the enhancements were associated with cumuliform clouds in dissipation stage while the cloud fringes were crossing over the Sun disk. Both attenuations and enhancements present spectral dependence: the first decreasing and the second increasing toward longer wavelengths. Typical magnitude of the enhancement of 1-min averages for PAR is close to 20%, with highest values exceeding 40%, and decreasing to 6% for 305 nm. Cases with well-defined cloud side reflections were not observed. A weak relation between cloud cover and enhancement magnitude was found: Larger cloud cover was associated with higher enhancements.

Citation: Lovengreen, C., H. A. Fuenzalida, and L. Videla (2005), On the spectral dependency of UV radiation enhancements due to clouds in Valdivia, Chile (39.8°S), *J. Geophys. Res.*, *110*, D14207, doi:10.1029/2004JD005372.

1. Introduction

[2] Clouds, together with solar zenith angle (SZA) and total ozone amount, are the most important factor influencing ground-level UV radiation. The importance of the UVB subregion (280–320 nm) derives from the well-known adverse effects on human health and living organisms in general. Most of the time, clouds attenuate the incoming solar radiation depending on cloud cover, altitude, and morphology. As far as the spectral variation, it has been shown that attenuation is wavelength-dependent, with cloud transmission slowly decreasing for larger wavelengths [*Seckmeyer et al.*, 1996; *Kylling et al.*, 1997]. However, scattered clouds can also increase UV radiation (UVR) locally. During the last several years, there has been considerable research on the UVR enhancement, stressing total ozone depletion but not UVR enhancements under scattered cloudiness or due to successive reflections between the cloud base and the ground. *Mims and Frederick* [1994] reported increases of 25% over the expected clear-sky value at 310 nm at Mauna Loa Observatory with a likely 1-min sampling interval. They warned that cumuliform clouds near the Sun disk could increase UVB global radiation, especially during summer high-Sun conditions, so protective measures should be taken even during cloudy days. *McCormick and Suehrcke* [1990] suggest that enhancement strongly depends on cloud type.

[3] The first studies on UV enhancement were carried out with broadband instruments [*Sabburg and Wong*, 2000; *Estupiñán et al.*, 1996]. Using 5-min averages, *Sabburg and Wong* [2000] and *Estupiñán et al.* [1996] reported erythemal UVB enhancements over 20%, with largest increases exceeding 26% in cases where the sky was covered more than 80% by clouds. Recently, *Cede et al.* [2002] reported observations from the Argentinean broadband network, including UV and global radiometers. These authors related enhancements and attenuation to SZA, cloud cover, and height. Irradiance enhancements were more pronounced from 5 to 7 oktas for cloud coverage and can last even hours, with peak instantaneous values of 13% for erythemal doserate and 33% for global irradiance. Enhancements under a broken cumulus cloud field were considered to be due to reflections on the cloud's sides.

[4] Few investigations have dealt with enhanced UV spectral data [*Schafer et al.*, 1996; *Sabburg et al.*, 2003].

0148-0227/05/2004JD005372

This is probably because of the higher cost and maintenance of properly calibrated spectral UV instruments but also because of the difficulty in obtaining uncontaminated scans by fast cloud variations during the scanning time (3–15 min), making it difficult to establish enhancements of spectral composition and duration.

[5] On the basis of a 3-min sampling interval with a Brewer MKIV spectrophotometer, *Schafer et al.* [1996] found only 17 integrated UVB measurements that surpass the expected clear-sky values in a 6-month period. Enhancements over a clear-sky expected value for the 290–320 nm interval were in the range of 1–11% for cloud cover between two and nine tenths. *Schafer et al.* [1996] showed that this occurred for the Sun disk partially obscured (DPO), excepting three cases with the Sun disk not obscured (DNO), and that most of the cases of derived UVB enhancements occurred under cumuliform cloud. *Sabburg et al.* [2003] made a comparison between spectrally determined UV (over 6-min scans) and broadband UVB and UVA enhancements at Toowoomba, Australia, taking in consideration different SZA. They used clear-sky irradiances as reference, and to avoid scans with cloud flagging, they included only cases with UVA and UVB enhancements in the same scan. They found that for wavelengths above approximately 306 nm the enhancements are wavelength-independent for all SZA with a ratio of the greatest to smallest enhanced irradiances of 1.2 in the UVB and the UVA. The enhancements reached maximum values of 30% and 50% for spectral UVA and spectral UVB, respectively. In previous work they had found maximum enhancements of 10%, whether for broadband UVA or for broadband UVB. With the exception of the SZA range centered on 20°, they found an increasing dependency with shorter wavelengths below 306 nm. For SZA of 32° and 42°, there were no enhancements for wavelengths above 306 nm until 363 nm (upper limit of the scan spectral interval).

[6] In this study we aim to establish the frequency of occurrence of summer enhancements in the UV and visible ranges at Valdivia, Chile, to determine their magnitudes and to characterize their spectral composition. Simultaneous collection of sky images allows a preliminary analysis of how cloud cover fraction, cloud type, and solar disk position influence the enhancements. The UV radiation regime at Valdivia, with its characteristic daily and annual variations, was the subject of a previous study by *Lovengreen et al.* [2000, 2002].

[7] To perform detailed studies of the spectral composition and duration of enhancements, a multiband filter radiometer was used, providing simultaneous 1-min averages of global irradiance at four UV wave bands and photosynthetically active radiation (PAR). Radiometers of this type partly avoid problems with cloud variations and stability within the scan duration. Further, instrument calibration was of secondary importance, referring enhancements to a clear day.

2. Experimental Setup, Data, and Methods

2.1. Radiation Data

[8] Data of UV and visible radiation collected with a filter radiometer GUV-511 (Biospherical Instruments) installed with a quasi-ideal horizon for the instrument at the roof of the Faculty of Science of the Universidad Austral de Chile (Valdivia, 40°S) were used for this study. The radiometer has four channels at the UV region, centered at wavelengths 305, 320, 340, and 380 nm with full width at half maximum $\cong$ 10 nm. A fifth channel measures total visible radiation (PAR). On the basis of measurements of the UV channels the erythemal doserates were estimated by means of a linear regression formula recommended by the manufacturers and depending on 305, 320, and 340 nm irradiances. Every minute, the instrument records the average of about 200 measurements, providing information of fairly rapid variations of clouds. Sensor stability is verified with a lamp set once a month, and once a year a comparison is made against an SUV-100 spectroradiometer located beside the GUV radiometer and a rover GUV calibrated by the factory. The SUV-100 has daily internal checks for wavelength and overall stability. Twice a month, absolute calibrations are performed using external calibrated lamps (calibrated by National Institute of Standards and Technology or by Optronics).

[9] Several summer months of data (see Table 1) taken during a 6-hour interval centered at solar noon (from 1400 to 2000 UT) were used. Solar zenith angle (SZA) at noon ranged from 16° to 50° from February to November. A summary of collected data is presented in Table 1.

2.2. Clear Days as a Reference for Changes

[10] For wave bands not affected by ozone (PAR, 380 nm, and 340 nm) or barely affected by it (320 nm), the enhancements and attenuations of irradiances were calculated using clear-sky values obtained from nearby cloud-free days occurring in the 3-year period. Because of the influence of the interdaily ozone variations on 305 nm irradiance and the erythemal doserate, such procedure could not be used to get reference values; instead, partly cloudy days were used to fit a polynomial to cloud-free periods, assuming that total ozone remained constant during the full day. This method also proved to be useful for other channels.

2.3. Images From the Sky and Their Analysis

[11] Sky images were taken every 2 min with a digital camera, AGFA ePhoto-1280, facing a horizontal convex mirror (30-cm curvature radius and a 20-cm diameter). Hence pictures were taken with half the frequency of irradiance measurements. This setup, with the camera at 30 cm over the mirror, allowed an amplified field of view of the sky up to an apex full angle of 120°.

[12] Software was developed to train a multilayer neural network [*Muller and Reinhardt*, 1995] with 50 patterns of RGB triplets associated to clear-sky and cloudy conditions. Since the original images were obtained on the spherical surface of the mirror, a procedure to get a "flat" version of the sky was also developed, associating the proper weight to each discrete element of the image. Then these tools were combined into an application that allowed the automatic recognition of cloud cover in the field of view of the images. Additionally, a tool was developed to determine whether each image corresponded to direct or diffuse radiation condition. Cloud types were determined from visual appearance. Relative position between Sun and cloud was recorded in three categories: Sun disk not obscured

Table 1. Summer Months Included in the Sample Indicating the Total Number of Days

	Summer 1999–2000			Summer 2000–2001				Summer 2001–2002				Total			
	TD[a]	PC[b]	P[c], %	TD[a]	PC[b]	P[c], %	IS[d]	TD[a]	PC[b]	P[c], %	IS[d]	TD[a]	PC[b]	P[c], %	IS[d]
November				30	21	5.5		30	19	7.4	5	60	40	6.4	5
December				31	7	2.0		31	5	1.6	7	62	12	1.8	7
January	31	20	6.2	31	17	4.4	6	31	6	1.2	2	93	43	4.0	8
February				29	15	3.8	4	28	9	2.4	2	57	24	3.1	6
Total												272	119	3.8	26

[a]Total days of the month.
[b]Partial cloudy days with enhancements.
[c]Probability of enhancement occurrence.
[d]Days with sky images.

(DNO), disk partially obscured (DPO), and disk obscured (DO).

2.4. Case Selection

[13] Analysis of the enhancements was done for days in November, December, January, and February in the summer periods indicated in Table 1, giving a total universe of 272 days. The number of days where at least one enhancement of PAR, 380 nm, 340 nm, and 320 nm took place is shown, summing up a total of 119 days with a total of 1096 events of enhancement. Because sometimes obtaining a reference clear day was difficult, the analysis of enhancements at 305 nm and for erythemal doserate was done only on 49 and 30 days, respectively.

[14] Only 26 days with enhancement were illustrated with sky photographs, and the image-processing software proved unfit for images obtained prior to January 2001. Because the camera had to be started and stopped manually, no holidays and weekends were included. In addition, since the camera was not wet proofed, on days when rain was to fall or it was already raining, no pictures were taken. For all these reasons the image sequence has a partial overlap with enhancement occurrence. A large number of pictures taken contained no enhancement event.

[15] Because enhancements were always larger in the PAR channel, the selection criterion was based on its measurements. An enhancement event was selected when PAR irradiance was at least 10% higher than the corresponding clear-sky value. This procedure was extended to the analysis of enhancements of 305 nm and the erythemal doserate on those days when it was possible to get a reliable reference clear day. The 10% cutoff in PAR assures that shorter wavelengths, simultaneously measured, are also enhanced (actually, at 305 nm, only one case out of 391 had a negative result).

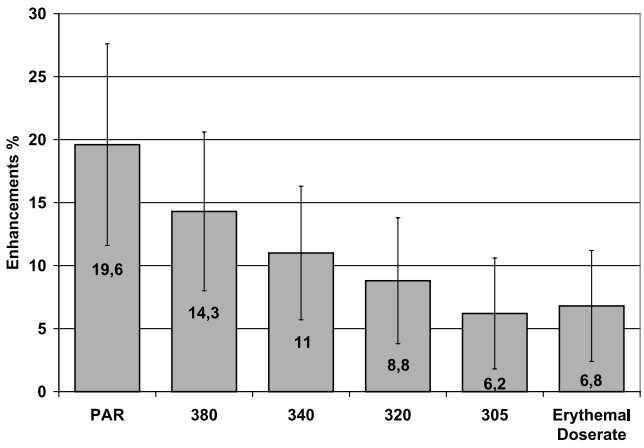

Figure 1. Average of enhancements (in percentages) for PAR; for 380, 340, 320 (N = 1096 cases), and 305 nm (N = 351 cases); and for erythemal doserate (N = 259 cases). Standard deviation bars are included.

3. Results

[16] From the 119 days with enhancements, for 49 days it was possible to include 391 simultaneous events in the 305 nm channel, and for 30 days, 259 events showed a rise of the erythemal doserate. Figure 1 shows the average value and standard deviation for the enhancement percentage with respect to a clear-sky condition. The largest magnitudes occur in the visible range with a mean of 19.6% (standard deviation = 7.7%), becoming smaller the shorter the wavelength. For the 305 nm channel the average enhancement was 6.2% (standard deviation = 4.2%). Maximum enhancements recorded were 50%, 38%, 32%, and 29% for PAR, 380 nm, 340 nm, and 320 nm, respectively.

[17] Frequency of occurrence of events for various intervals of enhancement fraction and each channel is given in Table 2. As expected, only 1.9% (21 events) of PAR enhancements exceeded 40% of clear-sky value, and most of the events were in the 10–20% interval. On the other hand, for 320 nm, only 35 cases (3.2%) exceeded 20% enhancement, and the largest number of events (67%) was under 10%. According to Figure 1, even less significant frequencies occurred for 305 nm and the erythemal doserate.

[18] With respect to event duration, Figure 2 indicates that short events occur more frequently. For all cases, 57.6% lasted at most 2 min, 20.2% lasted from 3 to 4 min, and only 6.4% of the 1096 cases exceeded 10 min.

[19] As an illustrative example of sky pictures taken, Figure 3 shows the typical graph obtained for 15 November 2001, from 1340 to 1730 UT, including enhancements and

Table 2. Percentages of Enhancements According to Their Magnitude (From 1096 Cases)

Enhancement, %	PAR	380 nm	340 nm	320 nm
>40	1.9			
30–40	8.4	2.2	0.4	
20–30	30.0	14.8	6.9	3.2
10–20	59.7	54.7	42.2	29.8

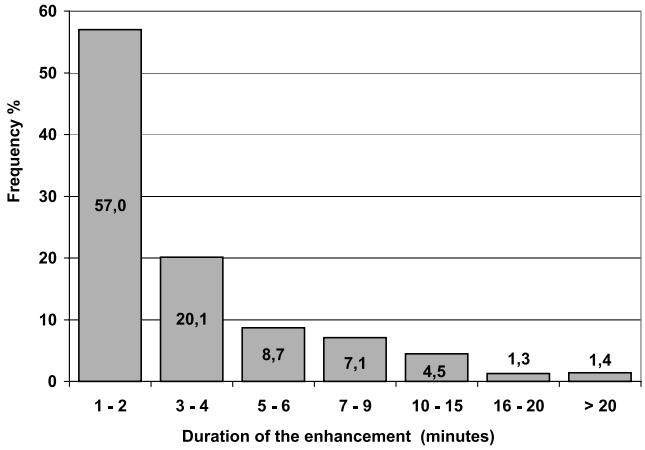

Figure 2. Frequency distribution of enhancements according to their duration.

attenuations of PAR, 380 nm, 340 nm, and 320 nm. Also shown are cloud cover fraction in percentage and transitions from direct to diffuse radiation and vice versa. The graph shows the spectral dependence of enhancements and attenuations. As already mentioned with reference to Figure 1, enhancements are always largest for the visible range, diminishing toward shorter wavelengths, that is, to more harmful wavelengths. Moreover, in the case of attenuations the spectral dependence of cloud effect is in the opposite sense: 320 nm is less attenuated than 340 nm, and this in turn is less attenuated than visible radiation. Figure 3 also shows that the transition from diffuse to direct radiation coincides (within 2 min) with the beginning of the enhancements, and the opposite transition (direct to diffuse radiation) coincides with the irradiance attenuation. It was verified that these transitions coincide with the condition DPO on most of the images: From 166 cases visually analyzed, 76.5% of the enhancements occurred under DPO conditions, 12.7% under DNO conditions, and 10.8% under DO conditions. This last, apparently contradictory, percentage can be understood as a result of several causes. First, the higher time resolution for irradiances (1 min) than for the image recording (2 min) permits the image to correspond to the previous or subsequent 1-min irradiance average. Second, there was a loss of synchronism between the computers connected to the camera and the radiometer. Finally, there is some uncertainty in determining the DO condition for cases with thin clouds.

[20] Figure 4 shows the typical cloud configuration which produces high enhancements; in this case, 30%, 24%, 20%, and 16% for PAR, 380 nm, 340 nm, and 320 nm, respectively. From the set of photographs available, Figure 5 shows the frequency distribution of enhancements by cloud type. Approximately 85% of cases are associated with cumuliform clouds at low and middle levels or a mixture of both. Some cirrus was present in 15% of all images.

[21] As far as cloud cover is concerned, a weak relation to enhancement magnitude was obtained: Highest rises were associated with at least 50% of cloud cover. This is shown

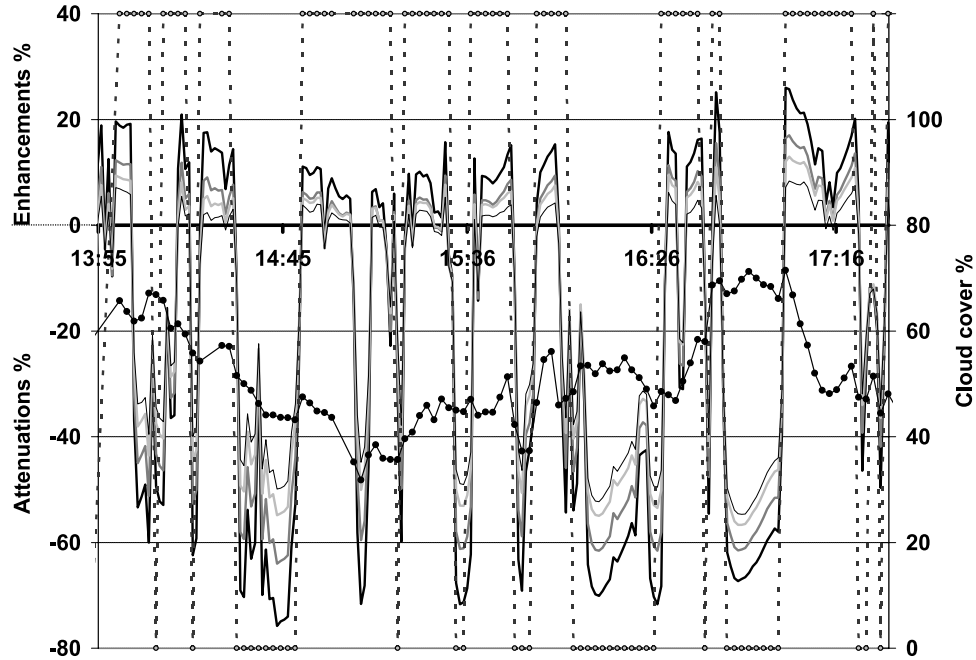

Figure 3. Case of 15 November 2001 showing enhancements and attenuations for PAR (thick black line), 380 nm (dark gray line), 340 nm (light gray line), and 320 nm (thin black line). Solid circles represent cloud cover percent, open circles at the bottom margin of the plot represent diffuse radiation condition, open circles at the top margin of the plot represent mostly direct radiation condition, and dashed vertical lines represent transitions.

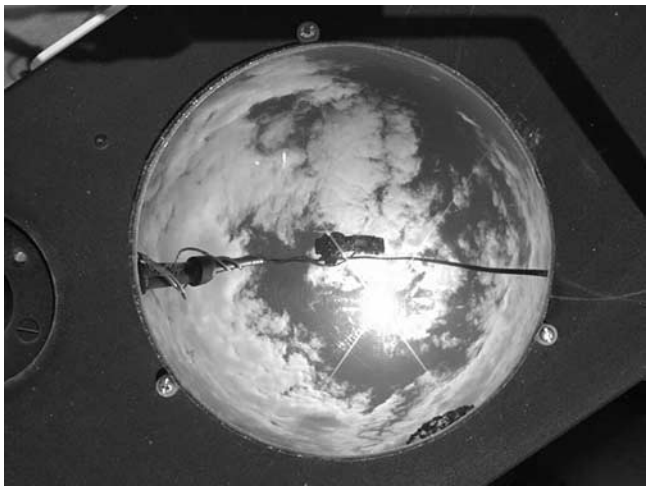

Figure 4. Image taken with the AGFA ePhoto-1280 on 27 November 2001 at 1535 UT showing a typical cloud configuration that produces high enhancements. Enhancements were 30%, 24%, 20%, and 16% for PAR and for 380, 340, and 320 nm, respectively. See color version of this figure in the HTML.

in Figure 6, where PAR enhancements over 30% occurred with 70% or more of coverage.

4. Discussion

[22] Previous studies of cloud enhancements of UV radiation have used single broadband radiometers or scanning radiometers. In the first case, there is no spectral discrimination, while in the second, there is a risk of cloud variations during the scan duration. This last shortcoming has particular relevance in the presence of shallow and scattered cloudiness, as seems to be the most frequent case for enhancements by cumuliform clouds. A multichannel radiometer represents a compromise between both, since there is some spectral resolution, but all wavelengths are sampled simultaneously. Therefore this is an important difference between this and previous studies, since this

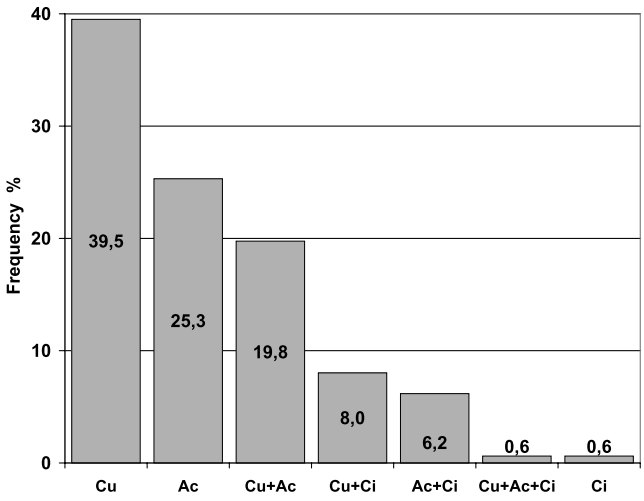

Figure 5. Frequency distribution of enhancements according to cloud type.

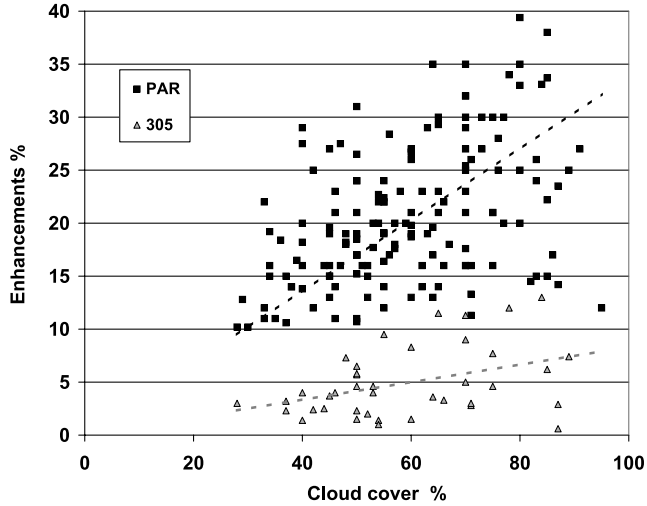

Figure 6. Scatterplot relating enhancements, for 305 nm and PAR, to cloud cover percentage. Regression lines are forced to pass through the origin.

study allows sampling of short-lived enhancements except for those under the 1-min averaging time. In summer at Valdivia, scattered cumulus occurs frequently during the diurnal phase of the sea breeze because of its proximity to the coastline. Furthermore, all cases were recorded during high Sun hours (within 3 hours of solar noon). The main results are summarized as follows.

4.1. Attenuation of UV Radiation and Visible Radiation at Surface Due to Clouds

[23] In relation to the attenuation of the UV and visible radiation due to clouds we obtained the same spectral dependence as previous authors, although some additional details in the UV range are presented here. Most authors compared total global radiation with UV radiation [*Blumthaler and Ambach*, 1988; *Dickerson et al.*, 1982;

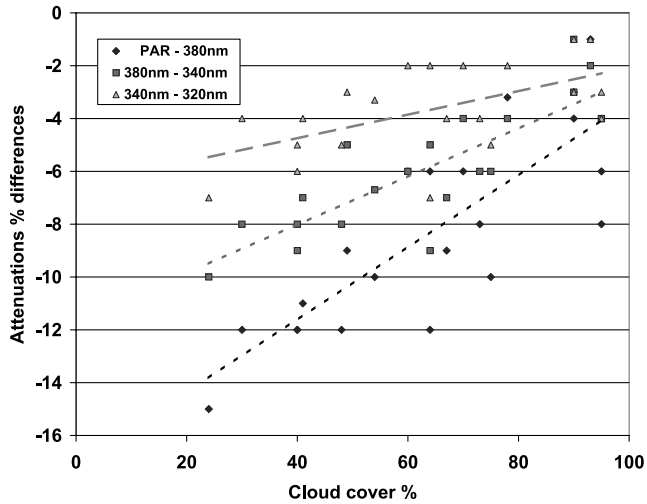

Figure 7. Attenuation difference (in percent) for wavelength intervals indicated as functions of cloud cover (percent), including corresponding regression lines.

Table 3. Enhancement Percent for 98th Percentile According to Our Data Evaluated With Average and Maximum Values for Each Enhancement and Results From *Cede et al.* [2002, Table 2]

	PAR	380 nm	340 nm	320 nm	305 nm	Erythemal Doserate
Average	34	26	21	18	14	15
Maximum	40	31	22	22	16	18
Cede et al. [2002]	35					13

Estupiñán et al., 1996; *Grant and Heisler*, 1999; *Josefsson and Landelius*, 2000]. *Schafer et al.* [1996], who measured reductions of UVB (280–320 nm) with a Brewer MKIV spectrophotometer as a function of cloud amount and SZA, obtained average UVB transmissions of 30% for overcast skies and 79% for the scans with four to five tenths of covered sky. As noted by *Josefsson and Landelius* [2000], these studies do not determine the true transmittance of clouds; it is better to refer to it as "cloud effect" since there are additional components in the measured radiation flux. Additionally, with a broken cloud layer, there will be interactions from the sides of the clouds.

[24] According to a set of 21 of the analyzed images, the spectral dependence of attenuations is larger with white cumuliform clouds, becoming weaker when the sky cover is more uniform, and almost negligible with complete cover. To illustrate the cloud cover dependence of attenuations such as those appearing in Figure 3, differences between sampled successive wavelengths (PAR to 380 nm, 380–340 nm, and 340–320 nm) are presented in Figure 7 as functions of cloud cover percentage. In spite of substantial scatter, regression lines indicate that the longer the wavelength, the higher the dependence on cloud cover and that this spectral discrimination becomes smaller as cloud cover increases. Since in this study the main focus is on enhancements rather than attenuations, days with full cover or rain are excluded. Clouds caused the largest attenuations on the visible wave band, reaching maximum reductions of 90% in PAR. In our data set, attenuations for 320 nm larger than 60% were unusual. In view of this spectral dependence, less attenuation is expected for even shorter wavelengths.

4.2. Enhancement of UV Radiation and Visible Radiation at Surface Due to Clouds

4.2.1. Spectral Composition

[25] The results indicate a systematic spectral composition of both enhancements and attenuations. Fractional enhancements are larger for longer wavelengths, while attenuations vary in the opposite sense: larger for shorter wavelengths. Most of the enhancements reported here occurred when the Sun was near cumuliform cloud borders. Such behavior does not agree with that reported from observations at Toowoomba, Australia, by *Sabburg et al.* [2003], who found larger increases at UVB than UVA. The same is valid with respect to a similar result by *Kylling et al.* [1997] in modeling the effect of a homogeneous cloud layer to explain observations by *Seckmeyer et al.* [1996] in Germany and finding a maximum enhancement at 320 nm on a cloud top.

4.2.2. Frequency of Occurrence and Duration

[26] Frequency distribution of enhancements decreases rapidly with duration, with 58% of them being shorter than 2 min, 20% shorter than 4 min, and 9% shorter than 6 min; only 2% lasted longer than 15 min. It has to be borne in mind that enhancements shorter than 1-min were not recorded because of the sampling interval.

4.2.3. Magnitude of Enhancements

[27] The average of enhancements, expressed as a percentage of clear-sky condition, varies smoothly from 6.2% for 305 nm to 19.6% for PAR with standard deviations of 4.2 and 7.7%, respectively. Most previous authors report enhancements for wide bands (UVA and UVB), making direct comparison difficult. However, by using 305 and 380 nm channels as representative of UVB and UVA, these results compare reasonably well with previously reported enhancements [*Estupiñán et al.*, 1996; *Schafer et al.*, 1996; *Sabburg and Wong*, 2000; *Cede et al.*, 2002; *Sabburg et al.*, 2003] except for a large (50%) enhancement in the UVB interval found by *Sabburg et al.* [2003]. Because of the large data set reported and geographical proximity, a comparison with *Cede et al.* [2002] deserves special attention. These authors report 98th percentiles for instantaneous enhancements measured at 15 min intervals for erythemal doserates measured with a UV biometer together with global solar irradiances measured with thermoelectric pyranometers at three locations in Argentina (from 22°S to 49°S). Table 3 includes the 98th percentile for our data set estimated with average and maximum values for each enhancement, together with *Cede et al.*'s [2002] combined data for the three sites.

[28] Agreement with *Cede et al.* [2002] results is surprisingly good considering instrument and sampling differences. In addition, their observations seem related to deeper convection to explain enhancements by cloud side reflection, while in our case the dominant cloud type was thin cumulus in dissipating stages. A substantial difference between both studies is in enhancement duration, which might be a consequence of either sampling rates or development stage of cumuli. For instance, in Figure 3, there are time intervals where an average enhancement over 15 min is made of several shorter enhancements. In our study this would count as two or three short-lived peaks instead of a single longer enhancement.

4.2.4. Other Factors

[29] In agreement with most of previous researchers we have found that cumuliform clouds and also the Sun disk not obscured or partially obscured conditions are important for enhancements. In this study the greatest enhancements occurred when a large portion of the field of view was covered with small clouds. This fact supports the comment by *Estupiñán et al.* [1996], who suggested that cloud coverage of 80–90% causes the greatest local UVB increases.

[30] In conclusion, under high-Sun conditions (summer and near noontime), substantial enhancements of UV radiation over short time intervals can be produced by drifting clouds. The spectral dependence is such that the shorter and more harmful irradiances present smaller percentage increases.

[31] **Acknowledgments.** The authors thank Maximiliano Valdebenito for his help in collecting and processing the irradiance measurements. This research was supported by IAI under project CRN-026 and project DID-UACh 2001-04.

References

Blumthaler, M., and W. Ambach (1988), Human solar ultraviolet radiant exposure in high mountains, *Atmos. Environ.*, *22*, 749–753.

Cede, A., M. Blumthaler, E. Luccini, R. Piacentini, and L. Nuñez (2002), Effects of clouds on erythemal and total irradiance as derived from data of the Argentine network, *Geophys. Res. Lett.*, *29*(24), 2223, doi:10.1029/2002GL015708.

Dickerson, R. R., D. H. Stedman, and A. C. Delany (1982), Direct measurements of ozone and nitrogen dioxide photolysis rates in the troposphere, *J. Geophys. Res.*, *87*, 4933–4946.

Estupiñán, J. G., S. Raman, G. H. Crescenti, J. J. Streicher, and W. F. Barnard (1996), Effects of clouds and haze on UV-B radiation, *J. Geophys. Res.*, *101*, 16,807–16,816.

Grant, R., and G. Heisler (1999), Estimation of ultraviolet-B irradiance under variable cloud conditions, *J. Appl. Meteorol.*, *39*, 904–916.

Josefsson, W., and T. Landelius (2000), Effect of clouds on UV irradiance: As estimated from cloud amount, cloud type, precipitation, global radiation, and sunshine duration, *J. Geophys. Res.*, *105*, 4927–4935.

Kylling, A., A. Albold, and G. Seckmeyer (1997), Transmittance of a cloud is wavelength-dependent in the UV-range: Physical interpretation, *Geophys. Res. Lett.*, *24*, 397–400.

Lovengreen, C., H. A. Fuenzalida, and L. Villanueva (2000), Ultraviolet solar radiation at Valdivia, Chile (38.8°S), *Atmos. Environ.*, *34*, 4051–4061.

Lovengreen, C., J. L. Alvarez, H. A. Fuenzalida, and M. Aritio (2002), Radiación ultravioleta productora de eritema en Valdivia: Comparación entre inferencias satelitales, modelo de transferencia radiativa y mediciones desde Tierra, *Rev. Med. Chile*, *130*, 17–25.

McCormick, P. G., and H. Suehrcke (1990), Cloud reflected radiation, *Nature*, *345*, 773.

Mims, F. M., III, and H. Frederick (1994), Cumulus clouds and UV-B, *Nature*, *371*, 291.

Muller, B., and J. Reinhardt (1995), *Neural Networks: An Introduction*, 1st ed., 344 pp., Springer, New York.

Sabburg, J., and J. Wong (2000), The effect of clouds on enhancing UVB irradiance at the Earth surface: A one year study, *Geophys. Res. Lett.*, *27*, 3337–3340.

Sabburg, J. M., A. V. Parisi, and M. G. Kimlin (2003), Enhanced spectral UV irradiance: A 1 year preliminary study, *Atmos. Res.*, *66*, 261–272.

Schafer, J. S., V. K. Saxena, B. N. Wenny, W. Barnard, and J. J. De Luisi (1996), Observed influence of clouds on ultraviolet-B radiation, *Geophys. Res. Lett.*, *23*, 2625–2628.

Seckmeyer, G., R. Erb, and A. Albold (1996), Transmittance of a cloud is wavelength dependent in the UV-range, *Geophys. Res. Lett.*, *23*, 2753–2755.

H. A. Fuenzalida, Departamento de Geofísica, Facultad de Ciencias Físicas y Matemáticas, Universidad de Chile, Blanco Encalada 2002, Santiago, Chile.

C. Lovengreen, Instituto de Física, Universidad Austral de Chile, Casilla 567, Valdivia, Chile. (clovengr@uach.cl)

L. Videla, Departamento de Ingeniería Matemática, Facultad de Ciencias Físicas y Matemáticas, Universidad de Chile, Blanco Encalada 2120, Santiago, Chile.